STABILITY OF RESIDUAL ACOUSTIC NOISE VARIANCE IN ACTIVE CONTROL OF STOCHASTIC NOISE

Iman Tabatabaei Ardekani and Waleed Abdulla

The University of Auckland, New Zealand

ABSTRACT

This paper concerns about the theoretical stability of the adaptation process performed by the Filtered-x Least Mean Square (FxLMS) algorithm in active control of acoustic noise. A dynamic model for the Variance of Residual Acoustic Noise (VRAN) is developed and it is shown that the stability of this model is a sufficient condition for the stability of the adaptation process. The basic rules governing the VRAN root locus are developed, based on which an upper-bound for the adaptation step-size is derived. This upper-bound can apply to a general case with an arbitrary secondary path, unlike the traditional upper-bound used in adaptive filter theory, which was derived only for pure delay secondary paths.

Index Terms— Active noise control, FxLMS algorithm.

1. INTRODUCTION

The general block diagram of a single channel feed-forward ANC is shown in Fig. 1. In this figure, $d(n)$ is the acoustic noise at the desired zone of silence, $x(n)$ is the reference signal measured by the reference microphone, $y(n)$ is the anti-noise signal generated by the ANC controller, and $e(n)$ is the residual acoustic noise measured by the error microphone in the zone of silence. The primary and secondary paths are shown by p and s, respectively. The secondary path impulse response coefficients $s_0, s_1, \ldots, s_{Q-1}$ must be identified in prior because they must be used by the FxLMS algorithm [1]. As shown, the response of the secondary path s to $y(n)$ is the anti-noise signal which is combined with the acoustic noise $d(n)$ at the desired zone of silence. The control signal $y(n)$ is generated by the ANC controller w which has a transversal digital filter structure (of order L). This structure is adjusted by the FxLMS algorithm. The mathematical equations describing the system are [2].

$$e(n) = d(n) - \sum_q s_q \mathbf{w}^T(n-q)\,\mathbf{x}(n-q) \tag{1}$$

$$\mathbf{w}(n+1) = \mathbf{w}(n) + \mu e(n) \sum_q s_q \mathbf{x}(n-q) \tag{2}$$

Thanks to the University of Auckland for supporting this research by a Faculty Research Development Fund).

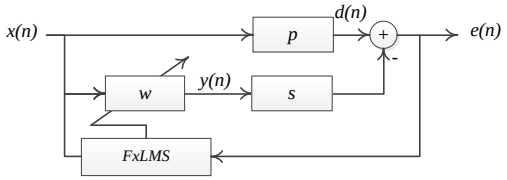

Fig. 1. Single channel adaptive feed-forward ANC

where q=0,...,Q-1 and the reference vector $\mathbf{x}(n)$ and the weight vector $\mathbf{w}(n)$ are given by

$$\mathbf{x}(n) = [x(n), x(n-1), \ldots, x(n-L+1)]^T \tag{3}$$

$$\mathbf{w}(n) = [w_0(n), w_1(n), \ldots, w_{L-1}(n)]^T \tag{4}$$

In [1], the *Rotated Weight Misalignment* (RWM) vector, $\mathbf{c}(n)$ is defined as

$$\mathbf{c}(n) = \mathbf{F}^T[\mathbf{w}(n) - \mathbf{w}_o] \tag{5}$$

where $\mathbf{w}_o$ is the optimal weight vector [3] and $\mathbf{F}$ is the modal matrix obtained from the diagonalization of the autocorrelation matrix $\mathbf{R}$=$E\{\mathbf{x}(n)\mathbf{x}^T(n)\}$ as $\mathbf{R}$=$\mathbf{F}\mathbf{\Lambda}\mathbf{F}^T$. The statistical expectation of $\mathbf{c}(n)$ can be interpreted as the first-order moment vector in the FxLMS adaptation process. In [4], the authors have shown that the dynamics of this vector corresponds to the following characteristic equation.

$$1 + \mu\sigma_x^2 \frac{\sum_q s_q^2 z^{-q}}{z-1} = 0 \tag{6}$$

where σ_x^2 is the power of $x(n)$. Also, it is shown in [4] that the roots of this characteristics equations are inside the unit circle if the step-size μ holds

$$0 < \mu < \frac{2}{\sigma_x^2 K} \sin\frac{\pi}{2(2D_{eq}+1)} \tag{7}$$

where K is a scalar given in [4] and D_{eq} is the secondary path equivalent delay:

$$D_{eq} = \left(\sum_q s_q^2\right)^{-1} \sum_q q s_q^2 \tag{8}$$

As shown in [4], the condition given in Eq. (7) is a necessary condition for the adaptation process stability. However,

whether this condition is a sufficient condition for the stability or not was left unanswered in [4]. This is the main question of this paper. This also clearly indicates the relationship between this paper and [4].

2. VRAN STABILITY

In adaptive filter theory, the FxLMS algorithm updates a digital filter, e.g. $\mathbf{w}(n)$, in such a way that the mean-square-error function $E\{e^2(n)\}$ is minimized. In view point of Acoustics, this function represents the power of the residual acoustic noise. In view point of Statistics, this function represents the *Variance of Residual Acoustic Noise* (VRAN) when the acoustic noise is a zero-mean signal: $E\{e(n)\}$=0. In [5], it is shown that this function can be expressed as

$$J(n) = J_0 + J_{ex}(n) \tag{9}$$

where J_0 is the minimal residual noise power and $J_{ex}(n)$ is the excess mean-square-error function. In [4, 6], the authors have shown that $J_{ex}(n)$ can be modeled by

$$J_{ex}(n+1) = \alpha J_o + J_{ex}(n) - \beta \sum_{p=0}^{Q-1} s_p^2 J_{ex}(n-p) \tag{10}$$

where σ_s^2 is the sum of squares of s_0,s_1,..., s_{Q-1} and scalars α and β are given by

$$\alpha = \mu^2 \sigma_s^4 \sigma_x^4 L \tag{11}$$

$$\beta = \mu \sigma_x^2 \left[2 - \mu \sigma_s^2 \sigma_x^2 (L + 2D_{eq})\right] \tag{12}$$

Based on Eq. (9) and (10), and considering this fact that VRAN is equal to $J(n)$, the following recursive equation can be obtained.

$$\sigma_e^2(n+1) = \left(\alpha + \beta\sigma_s^2\right) J_0 + \sigma_e^2(n) - \beta \sum_{p=0}^{Q-1} s_p^2 \sigma_e^2(n-p) \tag{13}$$

where $\sigma_e^2(n)$ denotes the VRAN function at time index n. The block diagram of this function can be plotted as shown in Fig. 2. This system is stable when all the roots of its characteristic equation are located inside the unit circle. This characteristic equation can be obtained from Fig. 2 as

$$1 + \beta \frac{\sum_q s_q^2 z^{-q}}{z-1} = 0 \tag{14}$$

The open loop transfer functions appeared in Eq. (14) is identical to the one appeared in Eq. (6). However, in Eq. (6) the static gain is equal to the step-size μ but in the new equation, the static gain is equal to β, which is a function of μ. Based on this result, it can be argued that the root locus of the VRAN dynamics is similar to the root locus of the RWM dynamics. However, the difference between the static gain (root locus scalar parameters) causes the stability conditions of the two systems to be different. This issue is studied in the following.

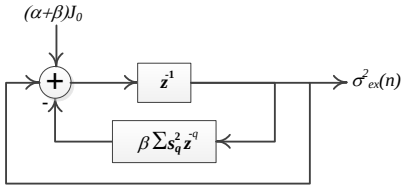

Fig. 2. Dynamic model for VRAN

2.1. VRAN Root Locus

The rules governing on the root locus of the RWM dynamics have been developed by the authors in [4]. Using these rules and considering the similarity between VRAN and RWM dynamics the following rules for plotting the VRAN root locus can be developed.

1. The VRAN root locus has Q branches. Hereafter, these branches are denoted by $B_1, B_2, ...$and B_Q.
2. B_1 starts at $z = 1$ and $B_2, B_3, ...$ and B_Q start at $z = 0$.
3. Assuming that the first Q_0 coefficients of the secondary path impulse response are zero, the VRAN root locus has $Q-Q_0-1$ end points but it has Q distinct branches. In this case, the other $Q_0 + 1$ branches approach one asymptote each.
4. The asymptotes originate from x_A and form the angles of $\varphi_k = \frac{(2k+1)}{Q_0+1}$ with the real axis.

$$x_A = \frac{1 + \left(\frac{s_{Q_0+1}}{s_{Q_0}}\right)^2}{Q_0 + 1} \tag{15}$$

5. The departure angle of B_1 is $\theta_1 = \pi$ and those of the other branches (B_qs) are $\frac{2(q-2)}{Q-1}\pi$.
6. The only interval on the positive real axis, which belongs to the VRAN root locus, is $(0, 1)$.
7. The root locus has a breakaway point given by

$$x_B = \frac{D_{eq}}{D_{eq} + 1} \tag{16}$$

2.2. VRAN Stability Condition

Based on the same logic used in [4], it can be shown that the roots moving on $B_1, B_2, ...$and B_Q are inside the unit circle if the root locus parameter (which is β here) is positive and smaller than a particular upper-bound U:

$$0 < \beta < U \tag{17}$$

$$U = \frac{2}{K_s} \sin \frac{\pi}{2(2D_{eq} + 1)} \tag{18}$$

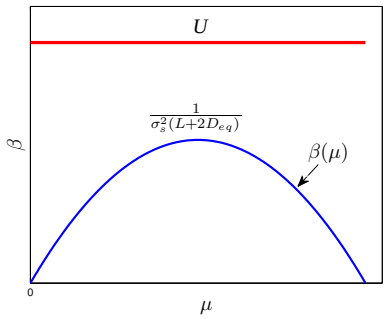

Fig. 3. Variation of β as a function of μ

As shown in Eq. (12), β is a function of μ. This function is plotted in Fig. 3. Maximizing this function results in

$$\max_{\mu} \beta = \frac{1}{\sigma_s^2 (L + 2D_{eq})} \tag{19}$$

This maximum point and the upper bound of U are also shown in Fig. 3. According to this figure ,

$$\max_{\mu} \beta \ll U \tag{20}$$

Combining this result and Eq. (17), one can show that the stability of the system requires only $\beta > 0$. For $\beta > 0$, Eq. (12) results in

$$0 < \mu < \frac{2}{\sigma_s^2 \sigma_x^2 (L + 2D_{eq})} \tag{21}$$

As a result, if μ holds Eq. (21), then the VRAN is stable. A similar stability condition was derived by the authors in [3] using a different stochastic analysis and with the aid of several independence assumptions about the acoustic noise. This paper derives this stability condition using the root locus theory. Note that the condition given in Eq. (21) can be considered as a sufficient condition for the adaptation process stability as the VRAN function can be considered as a Lyapunov function of the system variable. Also, note that Eq. (21) can apply to a general secondary path with the equivalent delay of D_{eq} while the traditional step-size upper-bounds given in [7, 8] can only apply to a pure delay secondary path with a physical time delay.

3. SIMULATION RESULTS

The existence of the step-size upper-bound (μ_{max}) proposed in this paper can be proved by using computer simulation. Fig. 4 shows the primary and secondary paths used in the simulation. A broad-band white signal with the power of σ_x^2=1 is used as the reference signal (noise). Fig. 5 shows the VRAN root locus of the simulated system. This plot obtained by using MATLAB, however, its parameters are in an excellent agreement with the theoretical findings given in Section

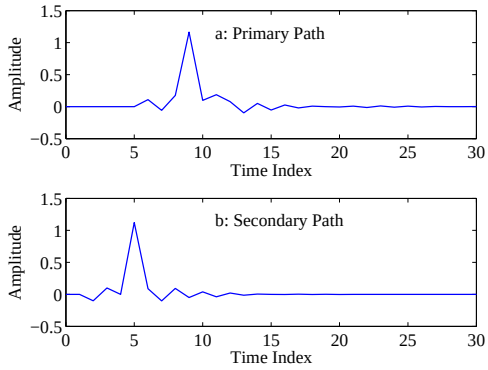

Fig. 4. Primary and secondary paths in computer simulation

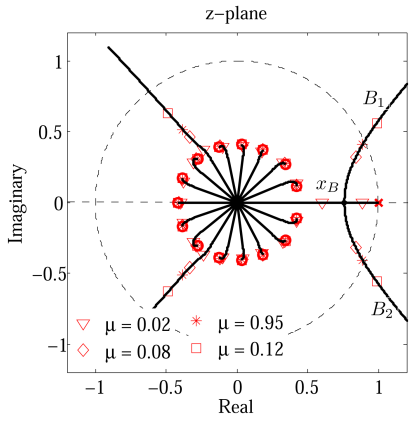

Fig. 5. Root locus of the simulated system

2.1. Fig. 6 shows the VRAN dynamics in the simulated system for three different step-sizes. It can be seen that when μ is set to 0.02 or 0.08, the system is stable but when it is set to 0.12, the system is unstable. Hence, μ_{max} should be between 0.08 and 0.12. This issue can be also seen in the root locus plot. The roots corresponding to μ=0.02 are shown by "∇" in Fig. 5. Also, the roots corresponding to μ=0.08 are shown by "$\diamondsuit$". As can be seen, in these two cases, all the roots are located inside the unit circle and, thereby, the system holds its stability. The roots corresponding to μ=0.12 are shown by "$\sqcap$". As can be seen, in this case, the roots moving on B_1 is located outside the unit circle; therefore, the system cannot holds its stability. The same behavior for the root located on B_2 is seen, as B_2 and B_1 are complex conjugates after reaching x_B.

In order to find a more accurate value for μ_{max}, more simulation experiments are conducted. μ is changed incrementally (e.g. with the incremental step of 0.001) until the system becomes unstable. For each μ, 100 independent simulation runs are repeated and the number of stable experiments is considered as the percentage of the stable experiments. The results can be plotted as shown in Fig. 7. According to this

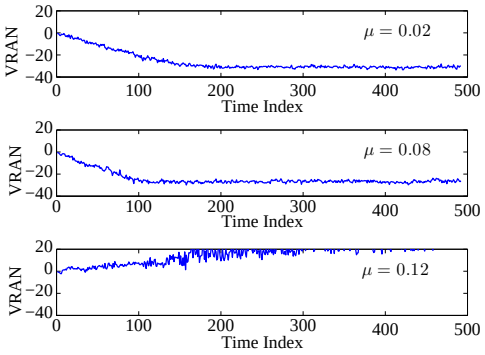

Fig. 6. VRAN for different step-sizes in computer simulation

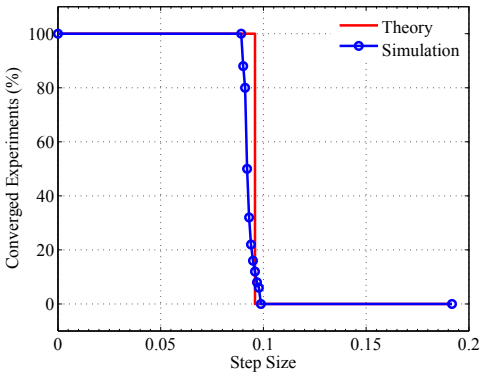

Fig. 7. μ_{max} obtained in theory and computer simulation

figure, when μ is below 0.089, all the simulation experiments are stable (μ_D=0.089) and when μ is beyond 0.099, there is no stable experiment (μ_U=0.102). Accordingly, it can be deduced that μ_{max} locates between μ_D and μ_U. To obtain a particular value, it is assumed that the actual μ_{max} is the average of these to values; thus, $\mu_{max} \approx 0.0955$.

On the other hand, a theoretical value for μ_{max} can be obtained by using Eq. (21). For the secondary path impulse response, shown in Fig. 4, D_{eq} can be computed by using Eqs. (8) as $D_{eq} = 3.0263$. Substituting these values and also substituting $\sigma_x^2 = 1$ into Eq. (21), the theoretical upper-bound for the step-size is computed as $\mu_{max} = 0.0971$. Comparing the two values of μ_{max}, obtained above, confirms the validity and accuracy of Eq. (21). In ideal conditions and for a perfectly accurate μ_{max}, it is expected that for step-sizes below μ_{max}, all ($\%100$) of simulation runs become stable and for step-sizes beyond μ_{max}, none ($\%0.00$) of simulation runs become stable. Fig. 7 shows the difference between this ideal expectation in theory and the results obtained from computer simulation. The agreement between the results is evident in this figure.

4. CONCLUSION

The root locus theory is found to be very efficient in the stability analysis of the FxLMS adaptation process in ANC systems. The rules governing the root locus of the VRAN dynamics in ANC are developed in this paper. These rules can be applied to plot the root locus of any FxLMS adaptation process performed in ANC systems. Based on this rule, the dynamics of the process can be studied and an upper bound for the adaptation step-size can be formulated.

5. REFERENCES

[1] S. M. Kuo and D. R. Morgan, *Active noise control systems: algorithms and DSP implementations*, Wiley Interscience, New York, NY, USA, 1996.

[2] I. Tabatabaei Ardekani, *Stability Analysis of Adaptation Process in FxLMS-based Active Noise Control*, Ph.D. thesis, The University of Auckland, New Zealand, 2012.

[3] I. Tabatabaei Ardekani and W.H. Abdulla, "Theoretical convergence analysis of FxLMS algorithm," *Signal Processing*, vol. 90, no. 12, pp. 3046 – 3055, 2010.

[4] I. Tabatabaei Ardekani and W.H. Abdulla, "On the stability of adaptation process in active noise control systems," *Journal of Acoustical Society of America*, vol. 129, no. 1, pp. 173–184, 2011.

[5] E. Bjarnason, "Analysis of the filtered-x LMS algorithm," *IEEE Transactions on Speech and Audio Processing*, vol. 3, no. 6, pp. 504–514, Nov. 1995.

[6] I. Tabatabaei Ardekani and W.H. Abdulla, "On the convergence of real-time active noise control systems," *Signal Processing*, vol. 91, no. 5, pp. 1262–1274, 2011.

[7] S.J. Elliott, I. M. Stothers, and P. A. Neslson, "A multiple error LMS algorithm and its applications to active control of sound and vibration," *IEEE Transactions on Acoustic, Speech and Signal Processing Processing*, vol. 35, pp. 1423–1434, 1987.

[8] S. J. Elliott, *Signal Processing for Active Control*, Academic Press, San Diego, CA., 2001.